

RESEARCH ARTICLE

The discovery of an *in situ* Neanderthal remain in the Bawa Yawan Rockshelter, West-Central Zagros Mountains, Kermanshah

Saman Heydari-Guran^{1,2,3*}, Stefano Benazzi^{4,5}, Sahra Talamo^{5,6}, Elham Ghasidian^{1,2}, Nemat Hariri^{2,7}, Gregorio Oxilia⁴, Samran Asiabani^{3,8}, Faramarz Azizi³, Rahmat Naderi³, Reza Safaierad⁹, Jean-Jacques Hublin^{5,10}, Robert A. Foley¹¹, Marta M. Lahr¹¹

1 Stiftung Neanderthal Museum, Mettmann, Germany, **2** Department of Prehistoric Archaeology University of Cologne, Cologne, Germany, **3** DiyarMehr Centre for Palaeolithic Research, Kermanshah, Iran, **4** Department of Cultural Heritage, University of Bologna, Bologna, Italy, **5** Department of Human Evolution, Max Planck Institute for Evolutionary Anthropology, Leipzig, Germany, **6** Department of Chemistry G. Ciamician, Alma Mater Studiorum, University of Bologna, Bologna, Italy, **7** Department of Archaeology, University of Mohaghegh Ardabili University, Ardabil, Iran, **8** Department of Architecture, Faculty of Art and Architecture, Bu-Ali Sina University, Hamedan, Iran, **9** Department of Physical Geography, University of Tehran, Tehran, Iran, **10** Collège de France, **11** Place Marcelin Berthelot, Paris, France, **11** Leverhulme Centre for Human Evolutionary Studies, Department of Archaeology, University of Cambridge, Cambridge, United Kingdom

* heydari-guran@neanderthal.de



OPEN ACCESS

Citation: Heydari-Guran S, Benazzi S, Talamo S, Ghasidian E, Hariri N, Oxilia G, et al. (2021) The discovery of an *in situ* Neanderthal remain in the Bawa Yawan Rockshelter, West-Central Zagros Mountains, Kermanshah. PLoS ONE 16(8): e0253708. <https://doi.org/10.1371/journal.pone.0253708>

Editor: David Caramelli, University of Florence, ITALY

Received: January 6, 2021

Accepted: June 11, 2021

Published: August 26, 2021

Peer Review History: PLOS recognizes the benefits of transparency in the peer review process; therefore, we enable the publication of all of the content of peer review and author responses alongside final, published articles. The editorial history of this article is available here: <https://doi.org/10.1371/journal.pone.0253708>

Copyright: © 2021 Heydari-Guran et al. This is an open access article distributed under the terms of the [Creative Commons Attribution License](https://creativecommons.org/licenses/by/4.0/), which permits unrestricted use, distribution, and reproduction in any medium, provided the original author and source are credited.

Data Availability Statement: All relevant data are within the paper.

Abstract

Neanderthal extinction has been a matter of debate for many years. New discoveries, better chronologies and genomic evidence have done much to clarify some of the issues. This evidence suggests that Neanderthals became extinct around 40,000–37,000 years before present (BP), after a period of coexistence with *Homo sapiens* of several millennia, involving biological and cultural interactions between the two groups. However, the bulk of this evidence relates to Western Eurasia, and recent work in Central Asia and Siberia has shown that there is considerable local variation. Southwestern Asia, despite having a number of significant Neanderthal remains, has not played a major part in the debate over extinction. Here we report a Neanderthal deciduous canine from the site of Bawa Yawan in the West-Central Zagros Mountains of Iran. The tooth is associated with Zagros Mousterian lithics, and its context is preliminary dated to between ~43,600 and ~41,500 years ago.

Introduction

Neanderthals were a very successful hominin lineage that existed for several hundred thousand years, and their extinction remains one of the most persistent questions in palaeoanthropology. With such a vast geographical range, which at times extended from westernmost Europe and across a very large area of Asia [1, 2] identifying the last surviving Neanderthal populations is critical for interpreting the mechanisms behind their demographic decline, the conditions that enhanced or reduced their resilience, and the geography and timing of their last interactions with modern humans. Unsurprisingly, one of the most controversial aspects of

Funding: Funding was provided from Deutsche Forschungsgemeinschaft (Grant 423897519) to SHG.

Competing interests: The authors have declared that no competing interests exist.

this debate is the chronology of their disappearance. Aspects of that chronology are relatively well established, in Europe, where Neanderthals appear to have a continuous occupation since the Middle Pleistocene, their last occurrence has been timed to ~ 40,000–37,000 cal. BP [1–4]. A number of sites testify to the presence of *Homo sapiens* in Europe from at least 46,000 BP—Bacho Kiro [1] and Grotta del Cavallo [5, 6]. Therefore, the chronology of Neanderthal extinction across most, if not all of Europe, implies a minimum of 4,000 years of contemporaneity with *Homo sapiens* groups [1, 2], during which both biological [7] and cultural [8] interactions took place. At the other extreme of their geographical range, the Neanderthal occupation of parts of Siberia reveals a very different pattern. Palaeoanthropological and ancient genomic evidence from Denisova, Chagyrskaya and Okladnikov caves suggests repeated west-to-east dispersals between 150,000 and 120,000 years [9–11] which gave rise to at least two temporary Neanderthal populations that became demographically vulnerable, characterised by episodes of interbreeding with local Denisovans and small population sizes [11–13].

However, there is one region that presents a particular challenge because of the sheer complexity of both its prehistoric record and its geographic setting—southwest Asia. Bordered by the Mediterranean Sea in the west and mountain ranges in the north and east, the core of the region consists of deserts and semi-deserts that, even during humid climate intervals, would have constrained resources along waterways [14]. Thus, the prehistoric record of southwest Asia is concentrated along an arc extending from the Levant in the west to the Caucasus in the north and the Zagros Mountains to the east. These areas—Levant, Caucasus and Zagros—in turn, offered hominins different challenges and opportunities, and this is reflected in their different records.

Biogeographically, the Levant oscillated between African and Eurasian biomes, acting as a temporary corridor for dispersing African populations [15]. It is now known that this corridor was used by *Homo sapiens* at least twice—between 177,000–194,000 years, as evidenced at the site of Misliya [16] and between ~120,000 and 90,000 years, as shown at the sites of Skhul and Qafzeh [17], before the area was permanently occupied by *Homo sapiens* around 55,000 years [18]. These intermittent early modern human occupations of the Levant were interspersed by the use of the area by Neanderthals [19], whose local extinction is represented by the last Middle Palaeolithic (MP) levels at Kebara at 48,000–49,000 BP [20]. However, the presence of *Homo sapiens* at Manot Cave ~55,000 years [18] suggests a relatively long period of overlap between the two groups in the area.

In contrast, the Caucasus, a 1200 km mountain range between the Black and Caspian Seas, was an important barrier to animal and hominin dispersals north, as shown by the genetic differentiation of several taxa into southern and northern Caucasus populations, and also reflected in differences in lithic technology [21,22]. Southern Caucasus MP assemblages appear to have been part of a Levantine network [21] that extended to the Zagros during the terminal MP phases [23]. However, in contrast to the Levant, Neanderthals occupied the Caucasus for nearly 10,000 years longer, with an age for the latest Neanderthal and MP industries similar to that of European Neanderthals, at ~ 40,000 cal. BP [22]. Yet, differently from both the Levantine and European records, *Homo sapiens* occupation of the Caucasus does not appear to occur prior to the local extinction of Neanderthals, thus suggesting no local contemporaneity of the two groups [22]. Ultimately, another picture of Neanderthal-*Homo sapiens* landscape interactions emerged from the Zagros Mountains which stretch over 1600 km in a northwest-southeast direction and reaching 4400 m above sea level (asl) in Iran. Moreover, due to the steep and rugged topographic conditions, the Zagros embrace diverse ecological ecotones. They represent a formidable geographical barrier, but also a diverse set of habitats and ecozones [24] that were exploited by hominins since the Lower Palaeolithic [25]. MP sites are relatively numerous, although only three have yielded Neanderthal fossils. The best-known of

these is Shanidar, where the remains of ten Neanderthals were discovered [26–28]. The Shanidar Neanderthals have played a major role in the discussions about the complexity of Neanderthal behaviour, both for the presence of older-aged individuals in the fossil assemblage and the controversial claims of a ‘flower burial’. Yet, despite their importance, their timing and contemporaneity have not been finely resolved; a broad age between 70,000 and 45,000 years has usually been reported, although recent excavations have suggested an age range of 55,000–45,000 years [28]. Approximately 350 km to the southeast, among a number of MP and UP sites, Wezmeh and Bisetun Caves in the Kermanshah region (Fig 1) have also produced Neanderthal remains. Wezmeh Cave has no artefactual evidence for human occupation in the Late Pleistocene, and the presence of a human premolar tooth (Wezmeh 1), recently shown to have Neanderthal affinities [29], was interpreted as the result of carnivore hunting/scavenging activities. The age estimation for this premolar is very poor, bracketed between 70,000 and 11,000 years based on the uranium-series analyses of the fauna by alpha spectrometry [29].

Nevertheless, the transitional period from Yafteh, Ghār-e Boof and Shanidar cave is bracketed between 45,100 and 40,350 cal. BP, with a 68.2% probability [30, 31]. Together with the approximate youngest age of the Neanderthal remains from Shanidar at 45,000 BP, this would suggest a pattern similar to the southern Caucasus, where modern humans succeed, rather than overlap in time with the local Neanderthals. Moreover, a probable, but undated, Neanderthal right proximal radius diaphysis was found in Bisetun Cave in association with typical Zagros Mousterian lithic artifacts [31, 32].

Despite these few Neanderthal fossil hominin remains, there is a widely held assumption that the MP assemblages in the Zagros Mountains were produced by Neanderthals, and that the local Middle to Upper Palaeolithic transition represents the arrival in the area of *Homo sapiens* [33]. Here we report the discovery of a new Neanderthal remain at Bawa Yawan rock-shelter (BY1) in the Central Zagros Mountains confirming that Neanderthals manufactured Middle Palaeolithic artifacts. The new chronology associate with the site in question is showing a surprising continuity of Neanderthals presence in the area long after the first Upper Palaeolithic *Homo sapiens*, however, more radiocarbon dates are on the way to strengthen our conclusions.

Materials and methods

All necessary permits for this research, including excavations and materials study to Saman Heydari-Guran, were issued by the Iranian Center for Archaeological Research (Permit number 963141/34/3952). The archaeological materials presented in this research are stored and available for the study with authorization from the Iranian Cultural Heritage and Tourism Organization (ICHTO) in Kermanshah Province.

The results for this study are based on the three excavation seasons between 2016–2018 in the archaeological site of Bawa Yawan (34° 38′ 23.70″N, 46° 55′ 48.36″E, 1300 m asl), locates in Kermanshah Region, Iran.

μCT images of BY1

"High-resolution μCT images of the lower deciduous canine BY1 were obtained with the following scan parameters: 125 kilovoltage (kVp), 120 μA, and 0.015 mm voxel size. The μCT volume was segmented using Avizo 9.2 software (Thermo Fisher Scientific, Waltham, Massachusetts, US), and the 3D models of the dental tissues (i.e., enamel, dentine and the preserved portion of the pulp chamber) were refined in Geomagic Design X (3D Systems Software, Rock Hill, South Carolina, US) to optimize the triangles and create fully closed surfaces.

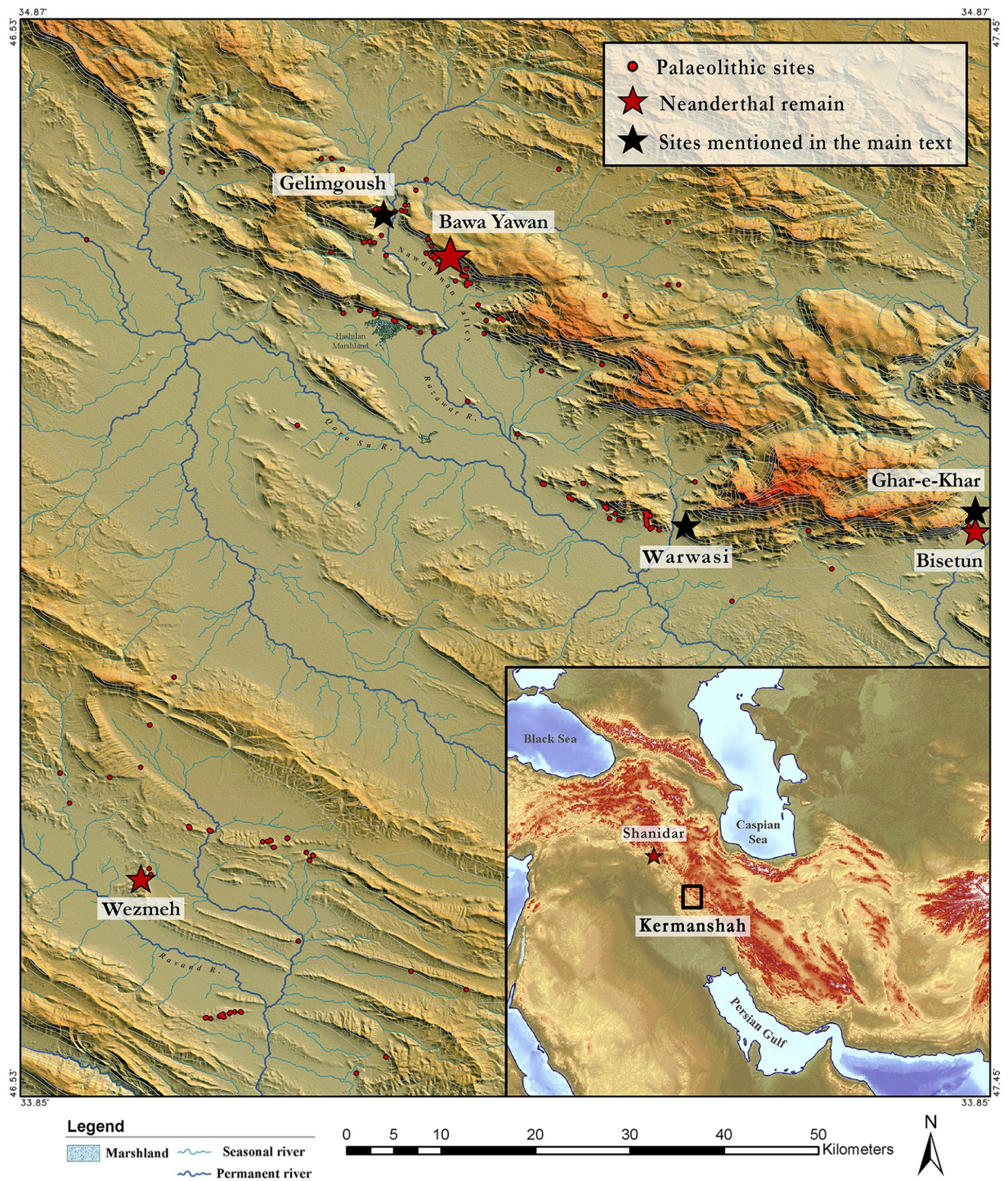


Fig 1. The inset map shows the location of the Kermanshah region in the Zagros Mountain. The main map shows the topography and hydrography of the Kermanshah region, the Bawa Yawan rockshelter in the Nawdarwan valley and the important sites mentioned in the text.

<https://doi.org/10.1371/journal.pone.0253708.g001>

The morphological description of BY1 was performed according to standards outlined by the (ASUDAS [34]) Although ASUDAS has been devised for modern human permanent dentition, we applied protocol to fossil deciduous tooth as already done in other publications [e.g., 35–37] because it permits a more precise and accurate comparison at each degree of

development. The wear stage of the occlusal surface was assessed based on [38], while the age of root resorption was estimated according to Moorrees et al [39, 40]. The crown diameters of BY1 were virtually measured in Geomagic Design X, orienting the tooth with the best-fit plane computed at the cervical line parallel to the xy-plane of the Cartesian coordinate system, and with the lingual aspect parallel to the x-axis. The size of the bounding box enclosing the crown was used to collect mesiodistal (MD) and buccolingual (BL) diameters.

Comparative data for the BL diameter was collected from the literature [40–42]. The computation of the 3D average enamel thickness (AET) and relative enamel thickness (RET) index follow [41]. A set of Neanderthals (NEA; $n = 6$), early *H. sapiens* (EHS; $n = 2$), and recent *H. sapiens* (RHS; $n = 3$) lower deciduous canines at different wear stages was acquired using a Skyscan scanner with voxel size ranging from 13 μm to 74 μm) at the Department of Human Evolution of the Max Planck Institute for Evolutionary Anthropology. As for BY1, dental tissues were segmented in Avizo 9.2 software, and the digital models were refined in Geomagic Design X. The 3D AET index (in mm) is the enamel volume divided by the underlying EDJ surface, while the 3D RET index (scale-free) is the 3D AET divided by the cube root of the crown dentine and pulp volumes.

Radiocarbon dating

Thirteen charcoal samples collected from GH 5, 4, 3, and 2 were submitted for ^{14}C dating to the Klaus-Tsichira-AMS facility of the Curt-Engelhorn Centre in Mannheim, Germany. Prior to dating, the samples were pretreated with the ABOX method and dated [43] in the radiocarbon lab. For samples that yielded finite conventional ages, calendar-year ages (and the corresponding 68.2% and 95.4% confidence intervals) were estimated using the IntCal20 calibration dataset [44].

Results

Nawdarwan Valley, Bawa Yawan rockshelter and stratigraphy

Located in the Nawdarwan Valley (34° 38' 23.70"N, 46° 55' 48.36"E, 1300 m asl), the Bawa Yawan (BY) rockshelter was discovered in 2009–10, during surveys for Palaeolithic sites in the Kermanshah region of the Central Zagros [33]. The Nawdarwan Valley forms a natural 17 km long corridor around the Razawar River that connects the two fertile plains of Kermanshah and Kamyaran in a N-S direction (Fig 1). The valley is rich in MP and UP rockshelters, with more than 50 sites identified during the surveys [33]. One of these, the Bawa Yawan rockshelter, is set in 50 m high limestone cliffs, visible from a far distance, that stand at the edge of a flat plain to the southwest (Fig 2A and 2B). A karstic spring, forming a natural pond, is located 50 m from the site. The archaeological deposits are accumulated on the southern slope of the cliff, occurring on a flat occupational area of ca. 300 m^2 , which is 10 m higher than the plain surface today. Several large boulders lie at the eastern corner of the rockshelter and on the talus slope, protecting the archaeological deposits from erosion (Fig 3A). Excavations of the Bawa Yawan rockshelter took place during three field seasons between 2016–2018. These focused on two areas, 10 m apart, both located close to the rockshelter wall, named the Western (14 m^2) and Eastern (6 m^2) trenches (Fig 3A).

The Bawa Yawan deposits are divided into 5 geological horizons (GH 1–5) based on colour and sediment texture (Fig 3C). These have a gradient of about 10° from the back wall towards the outside, but are relatively level in east and west directions (Fig 3A and 3B). The deposits are mostly composed of clastic materials, and fine sediments washed into the site through joints and bedding planes from the back-wall cliff. In some squares (H31, I31) the excavation reached a maximum depth of 4.5 m from the surface without reaching bedrock (Fig 3B and 3C). Some



Fig 2. A. Picture shows the Nawdarwan Valley and red arrow indicates the position of the Bawa Yawan rockshelter. B. Picture shows the Bawa Yawan cliff and excavation area.

<https://doi.org/10.1371/journal.pone.0253708.g002>

horizons, particularly GH2 and GH5, are characterised by a significant number of irregular stones collapsed from the cliff, varying in size from large boulders to small pebbles. GH3, with an average thickness of 80 cm, is different from the other geological horizons in being harder and having a higher carbonate content, protecting the underlying deposits from erosion.

- **GH5:** a dark reddish-brown (dry 5YR3/4 and moist 5YR2/4 very dark reddish-brown) and only exposed in five squares at Western trench and with 150 cm includes the lowermost geological layer and the deepest part of the excavation (Fig 3B and 3C). The sediments' colour becomes darker containing a lot of iron oxide particles, specifically in the lower part of the section. The deposits range from sandy/silty granules up to angular limestone of different sizes from small pebbles to boulders coming from the back wall of the shelter. The contact between GH4 and GH5 is gradual. The sediments become gradually reddish-dark brown downwards, specifically in the lowermost part of the section. It is the richest layer throughout the stratigraphy and is associated with numerous bone fragments which are partly burnt, very small charcoal fragments, and MP lithic artifacts of the Zagros Mousterian tradition. This GH yielded a good amount of fauna including *Bovidae*, *Bovidae antilopinae* and

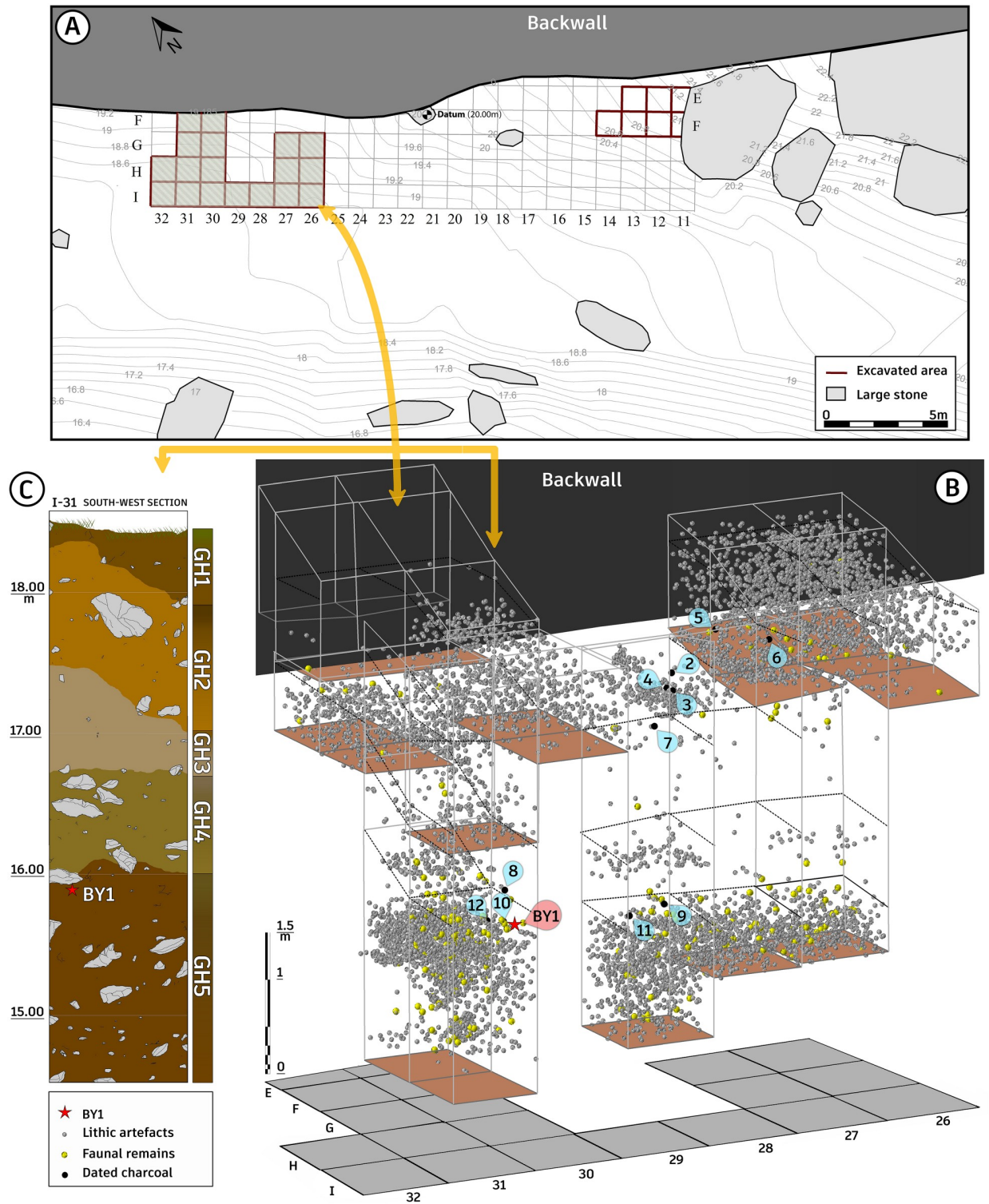


Fig 3. Bawa Yawan rockshelter. A. Topographic map and plan of the rockshelter showing the excavation area. B. 3D of the Western trench including position of BY1, dated charcoals, fauna and lithic artifacts. C. Profile shows the south-western wall of sq. I31, geological horizons and position of BY1.

<https://doi.org/10.1371/journal.pone.0253708.g003>

Equidae. So far, bedrock has not been reached during the three excavation seasons and at a depth of 4.70 m (Fig 3).

- **GH4:** This GH with about 65 cm thickness and a light reddish-brown colour (dry 5YR4/6 reddish-brown and moist is 5YR7/3 dull orange) stands in sharp contrast with the underlying horizon (GH5). The amount of angular cobbles and boulders is more than the upper GHs. This GH faces a dramatic decrease in cultural materials, indicating a sudden abandonment of the site. The few lithic artifacts recovered in this layer belong to MP period (Fig 3).
- **GH3:** Around 95 cm thick, the GH3, changes relatively gradually from GH4 (dry 5YR7/3 dull reddish-brown and moist 5YR ¾ dark reddish-brown). It contains light colour compacted highly calcareous deposits with concentration of ebbouls and angular pebbles. The number of lithic artifacts drops dramatically in this GH. Most of them are typical MP artifacts, some of which indicate Levallois technology. Very few UP artifacts have been also observed but only at the uppermost of GH3. The faunal remains are scattered and very fragmented as well (Fig 3B and 3C).
- **GH2:** This layer was observed in both Western and Eastern trenches. Up to 80–95 cm thick, GH2 is in general composed of reddish-brown deposits (dry 2.5YR5/4, moist 2.5YR2.5/3-dark reddish-brown) mixture of sand-silt-clay grain sediments associated with cobbles and medium-sized pebbles. This layer yielded archaeological materials from three different periods of MP, UP and Epipaleolithic (Fig 3B and 3C). GH2 yielded relatively abundant fauna, but highly fragmented including *Bovidae*, *caprinae*, and small birds.
- **GH1:** The uppermost geological layer is dull reddish-brown (dry 5Y6/4 dull orange, moist 2.5YR4/4, dullreddish-brown) and is around 30 cm thick, containing the recent soil associated with a few mixed modern objects and it is separated by an erosional unconformity to the underlying layer (GH2).

BY1 Neanderthal tooth. At a depth of around 2.50 m from the surface in the upper part of GH5, where the density of MP cultural materials gradually reduced, an *in situ* hominin tooth (hereafter called BY1) was recovered in association with fauna and Zagros Mousterian lithic artifacts (Fig 3B and 3C). The tooth is an exfoliated lower left deciduous canine (Ldc1) consisting of a relatively well-preserved crown and about one-fourth of the root (Fig 4). Neither caries nor enamel hypoplasia is visible. The enamel shows several longitudinal fractures from the cervix to the incisal surface that affect the underlying dentine. The incisal surface is worn obliquely, mesially to distally, exposing a large area of dentine up to wear stage 4 [38]. The buccal surface exhibits a mesiodistal convexity with its maximum at the mesial aspect (Arizona State University Dental Anthropology System (ASUDAS) grade 4). Accordingly, in the incisal view, the crown appears asymmetrical, which is further emphasized by the distal projection of a moderate lingual cervical eminence. The lingual surface is concave, bordered by moderately expressed distal and mesial marginal ridges (as also clearly shown in the EDJ, Fig 4). These ridges merge at the cervical eminence giving a semi-shovel shaped aspect to the crown (ASUDAS grade 4).

The moderate buccal bulging of the crown and the slight flaring of the mesial and distal sides from the cervix are more consistent with a lower than an upper deciduous canine. Interproximal wear facets are visible on both mesial and distal sides, the distal side being smaller (length: 1.20 mm; height: 1.73 mm) than the mesial one (length: 1.49 mm; height: 2.59 mm). The preserved root, slightly more elongated labially (mid-labial height: 2.95 mm) than lingually, (mid-lingual height: 2.31 mm) is resorbed (stage Res3/4 [45]), suggesting an age at exfoliation of approximately six years on the basis of recent human standards [38]. The crown has

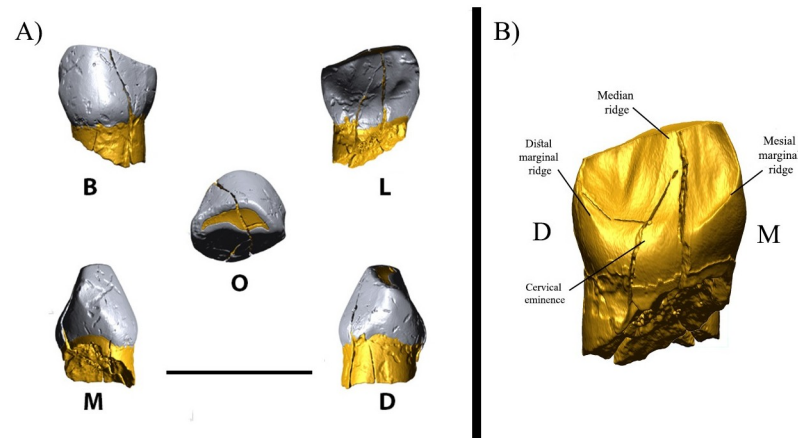


Fig 4. Lower left deciduous canine (BY1). A) BY1 in different views. B) The enamel-dentine junction of the tooth shows the cervical eminence and lingual ridges. Abbreviations: B: buccal, L: lingual, M: mesial, D: distal, O: occlusal.

<https://doi.org/10.1371/journal.pone.0253708.g004>

a mesiodistal (MD) diameter of 6.87 mm (minimum estimation due to wear) and a buccolingual (BL) diameter of 6.50 mm, which is close to UP *Homo sapiens* and, particularly, Neanderthal mean values (Table 1). At the cervix, the MD and BL diameters are, respectively, 5.32 mm and 5.88 mm. Despite the reduced comparative sample and the intrinsic limits due to the wear stage of the teeth, unworn Neanderthal lower deciduous canines show the average and relative enamel thickness indices (AET and RET respectively) lower than the values observed for worn early and recent *Homo sapiens* specimens (Table 2). The Z-scores computed for the AET and RET values of the BY1 specimen fall very close to the mean values of Neanderthals at similar wear stage (i.e., Krapina 51, Tagliente 4), further supporting its Neanderthal affinity.

Cultural materials and artefact technology and typology. The technological and typological characteristics of the Bawa Yawan artifacts are based on detailed studies of the lithic assemblages from GHs 5 to 2. Three techno-complexes of MP Mousterian, UP "LaK" [46] and the Epipalaeolithic from Bawa Yawan have been compared with their counterparts throughout the Zagros Mountains (Figs 5–7). We use attribute analysis and chaînes opératoire approaches to compare specifically the assemblages from the West-Central Zagros sites including Warwasi and Shanidar. Key attributes include core preparation and reduction strategies, degree of core reduction, modes of flaking, platform preparations, and the retouching and re-sharpening of the tools. We recorded the technological attributes of each artefact individually and in relation to the reduction sequence in order to reconstruct the chaînes opératoires in each archaeological horizon.

Table 1. Buccolingual (BL) crown diameter of BY1, compared to mean values of Neanderthal (NEA), early *Homo sapiens* (EHS) and recent *Homo sapiens* (RHS) lower deciduous canines.

Specimens	N	BL (mean±SD)	Z-score
BY 1		6.5	
NEA	23 ^a	6.0±0.5	1
UPHS	21 ^a	6.0±0.4	1.25
RHS	100 ^b	5.2±0.6	2.16

^a[42];

^b[40].

<https://doi.org/10.1371/journal.pone.0253708.t001>

Table 2. Values of the components of enamel thickness computed for Neanderthal (NEA), early *Homo sapiens* (EHS) and recent *Homo sapiens* (RHS) lower deciduous canines at different wear stages (ws).

Specimens	n	Wear stage	Ve	Vcdp	Sedj	3D AET	Z-score	3D RET	Z-score
BY 1		4	29.15	79.81	81.52	0.36		8.31	
NEA	4 ^a	1	37.32 (10.49)	75.31 (19.26)	86.39 (16.85)	0.43 (0.05)	1.4	10.17 (0.70)	2.66
	2 ^b	4	30.65 (4.07)	89.02 (1,34)	85.37 (1.21)	0.36 (0.05)	0	8.05 (1.22)	-0.21
EHS	2 ^c	3/4	39.37 (0.35)	77.73 (2.72)	83.33 (4.23)	0.47 (0.03)	3,67	11.09 (0.79)	3,52
RHS	3 ^d	2/3	32.58 (4.35)	53.94 (8.73)	64.54 (7.93)	0.51 (0.04)	3,75	13.23 (1.56)	3,15

Ve: enamel volume; Vcdp: crown dentine and pulp volume; Sedj: enamel-dentine junction surface; AET: average enamel thickness; RET: relative enamel thickness;

^aKebara 1, Kebara KMH4, La Quina_LQ32, Le Ferassie 8;

^bKrapina 51, Tagliente 4;

^cQafzeh 12, Qafzeh 15;

^dUlac 81, Ulac 140, Ulac 477 (from the Department of Human Evolution, Max Planck Institute of Evolutionary Anthropology)

<https://doi.org/10.1371/journal.pone.0253708.t002>

The excavations revealed three archaeological horizons throughout the stratigraphy, resulting in a total of 10,411 lithic artifacts (Tables 3 and 4); those artifacts that were in primary depositional context were concentrated in two dense bands in GH5 (MP) and GH2 (MP, UP and Epipalaeolithic) (Fig 3B). MP materials were recovered from GH3 and GH4, although at lower concentration levels. At the top of the sequence in the Eastern trench, close to the rockshelter wall, there is a rich Epipalaeolithic industry, similar to that reported at the Warwasi rockshelter [47], characterised mainly by geometric microliths and microburins. Following the Epipalaeolithic, the first half of GH2 in both the Eastern and Western trenches preserves UP lithics typical of the West-Central Zagros, especially in Warwasi [46]. The lithics are characterised by laminar technology. The tools mainly dominated by different kinds of twisted and retouched bladelets and end scrapers. At the bottom of GH2, and throughout GH3 to GH5, in both the Eastern and Western trenches, lithics typical of the MP Zagros techno-complex, namely the Zagros Mousterian [48], were uncovered (Tables 3 and 4, Figs 5 and 6).

Chronology. Thirteen charcoal samples were collected from different parts of the Bawa Yawan stratigraphy: (a) six charcoal samples were obtained from the below and above the hominin tooth in GH4 and GH5; (b) six samples from squares I29 and G27 from the beginning and middle of the UP occupation in GH2 and GH3; (Fig 8) (c) and one sample from the Epipalaeolithic layer at the upper part of GH2 in the Eastern Trench.

Eight of the twelve samples were successfully dated, while one returned a minimum date (Tables 5 and 6). All the ¹⁴C results are calibrated using the new IntCal20 [43] within the OxCal 4.4 program [43, 49] and are discussed here at 68.2% probability. The youngest occupation of the site, corresponding to the Epipalaeolithic level, ranging between 13,400 and 13,300 cal. BP (Fig 9) Only two of the six charcoal samples from the UP GH2 were dated successfully (both from square G27: MAMS-41723 and MAMS-41725). The two ages obtained are consistent with each other, yielding calibrated age ranges of 34,700–34,400 and 34,600–34,400 cal. BP, respectively (Fig 3B and Table 5). Five of the six charcoal samples collected from MP occupation layers (GH4 and GH5) produced reliable radiocarbon ages; a fifth sample produced a minimum age. (Table 7 and Fig 8). The ages obtained are consistent with their respective depths within the stratigraphy. The sample from the middle part of GH4 (MAMS-44523), 30 cm above the level of the BY1 in the same square (I31), provided an age of 40,300–39,400 cal. BP. Another sample from square I31 (MAMS-44525), at 9 cm above BY1, provided an age between 42,100 and 41,800 cal. BP, and a charcoal sample at a level just 2 cm above BY1 in square H31 (Beta-465001) provides the closest age estimation of the specimen, ranging between 43,000 and

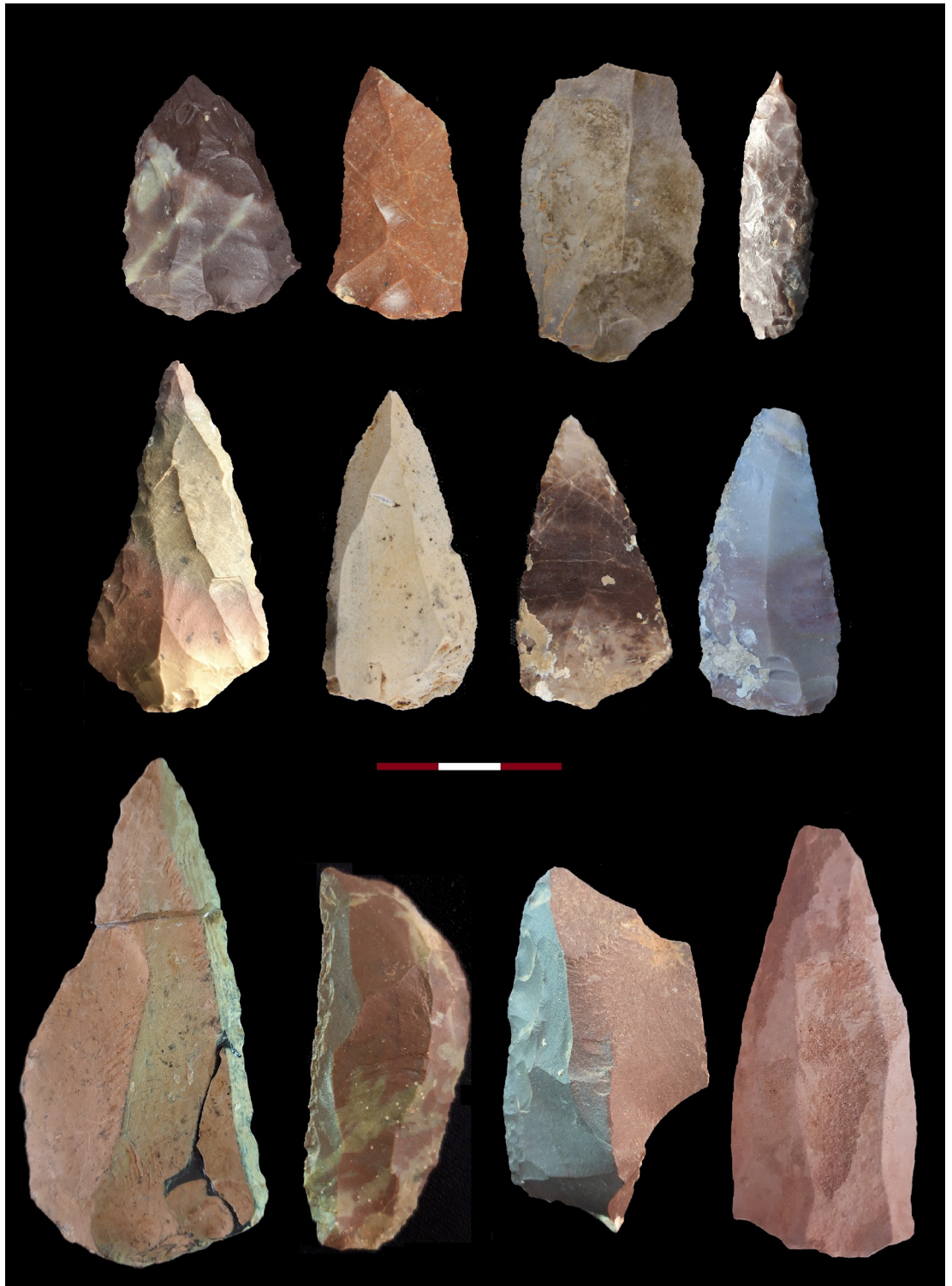


Fig 5. 1, 5, 7–9. Convergent scraper, 2,3,6,12. Levallois flake, 4. Limace, 10. Double scraper, 11. Single scraper.

<https://doi.org/10.1371/journal.pone.0253708.g005>

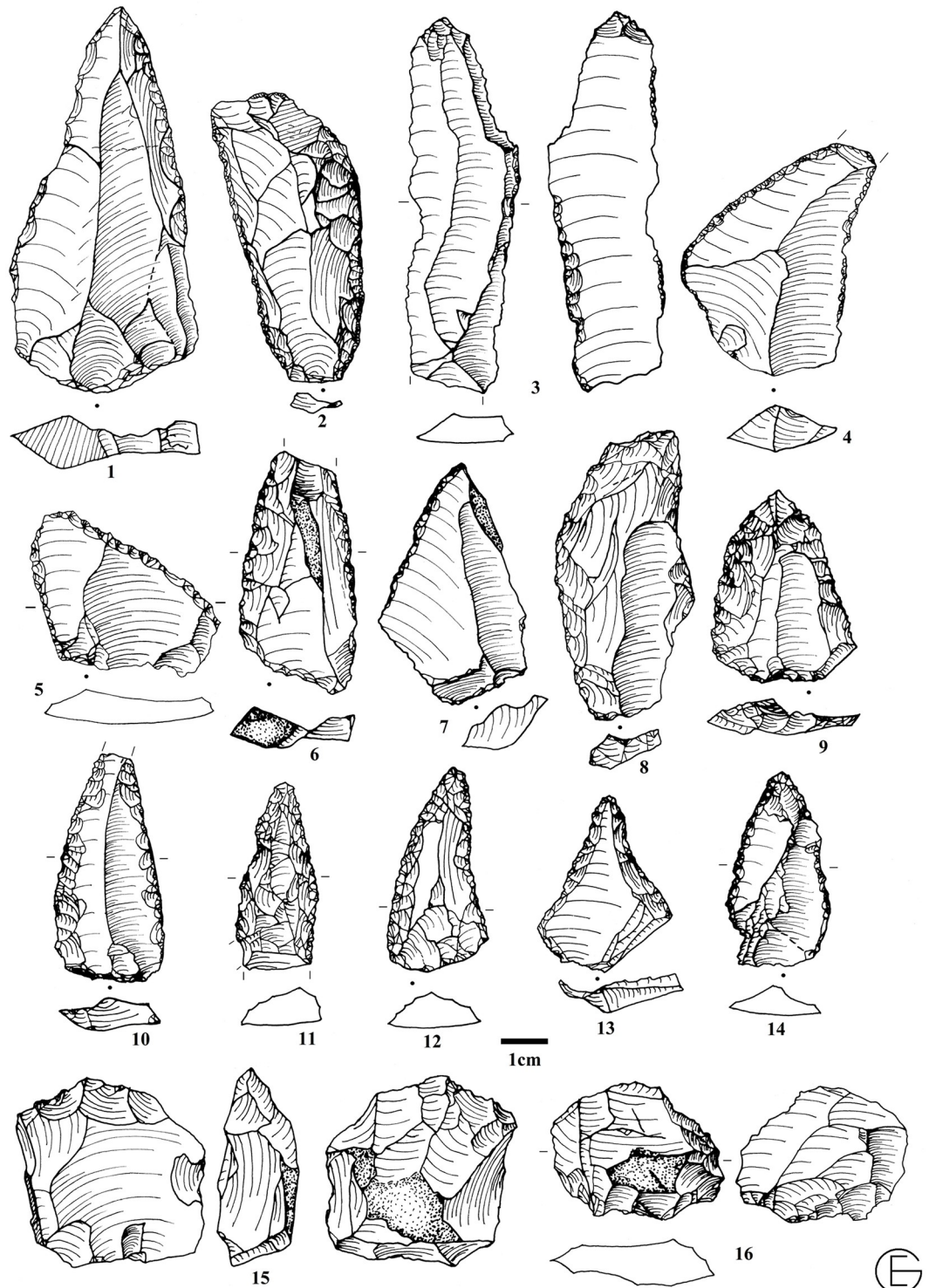


Fig 6. A sample of the Zagros Mousterian artifacts from the Bawa Yawan rockshelter around the BY 1. 1, 9–14. Convergent scraper, 2, 6. Double scraper, 3. Denticulate, 4, 5. Dejeite scraper, 7. Single scraper, 8. Scraper, 15, 16. Truncated faceted.

<https://doi.org/10.1371/journal.pone.0253708.g006>



Fig 7. A: 1. Platform bladelet core, 2, 3. points on bladelet, 4, 5. Geometric microliths, 6,7. Retouched bladelets. B: 1. platform bladelet core, 2. Denticulated bladelet, 3, 4. Twisted bladelets, 4, 5. Retouched twisted bladelets.

<https://doi.org/10.1371/journal.pone.0253708.g007>

42,500 cal. BP. The MAMS-41724 sample, 9 cm below the level of BY1 in square I29, provided an age range of 44,100–43,200 cal. BP, while a charcoal sample (OxA-36752) 11 cm below the level of BY1 in square H31 provided an age older than 44,200 BP dating range. (Table 7).

We performed a Bayesian model using the new IntCal20 in OxCal 4.4 and the t-type outlier analysis (prior probability set at 5%), to detect if there is any problem between the ^{14}C ages and their relative stratigraphic position at the site (Fig 9 and Table 6). The model, which was run

Table 3. All lithic artifacts from the west trench.

Z	Flake	blade	bladelet	core	tool	AD	SD/MD	sum
20.8–20.89	2	2	1		3		2	10
20.7–20.79	19	8	12	1	6		33	79
20.6–20.69	38	13	25		7		3	86
20.5–20.59	157	43	97	2	40	5	326	670
20.4–20.49	188	72	148	5	46	11	213	683
20.3–20.39	49	23	42	1	11	1	53	180
20.2–20.29	68	27	40		12	4	29	180
20.1–20.19	114	7	32		7	4	25	189
20.0–20.09	75	5	16		2	2		100
19.9–19.99	9	1	5				8	23
19.8–19.89	8	3	3			1	14	29
19.7–19.79	4	1	7		1		13	26
19.6–19.69	2		1					3
19.5–19.59		1	1					2
Sum	733	206	430	9	135	28	719	2260

The lithic artifacts are divided into technological categories based on artificial 10 cm spit. AD: angular debris, SD: small debitage (> 10mm), MD: micro debitage (> 5mm).

<https://doi.org/10.1371/journal.pone.0253708.t003>

using only the dates from GH5 until the GH2, confirm the integrity of the chronology with an Agreement index of 107%, well above 60% (Table 7 and Fig 8). The layer GH5 start at 44,600–43,100 ending in a transitional boundary with the GH4 at 42,000–40,500 cal. BP. In reality, one ^{14}C age at the bottom of the sequence, result in an age older than 44,200 ^{14}C BP, hence it could be older than the ages provided by the Bayesian model. Using the ‘date’ command in OxCal we estimated the duration of each phase at the site, and knowing the exact stratigraphic depth of the Neanderthal tooth in relation with all the others samples, an indirect date of BY1 could have been determined (see Method section). The total duration of GH5 ranges between 43,600 and 41,500 cal. BP, the duration of GH4 is between 41,100 and 39,000 cal. BP, with the upper part (GH2) ranging between 34,900 and 34,200 cal. BP (Table 7).

These dates indicate that the Bawa Yawan rockshelter contains a sequence from the MP to the UP in both the Western and Eastern trenches, as well as an Epipalaeolithic occupation level above those in the Eastern trench, which was not modelled. According to the Bayesian age modelling, GH4 and GH3 are broadly simultaneous with a substantially cold period in the Northern Hemisphere—the so-called Heinrich Stadial 4 (Fig 8), which might be responsible for the reduced cultural materials in this GH.

Furthermore, at this stage of research, these ranges show two critical ages for the Neanderthal occupation of the Zagros Mountains—first, the age of the Neanderthal BY1 tooth can be bracketed between 43,600 and 41,500 cal. BP, and second, the possible age of a young Zagros Mousterian in the area around 39,000 cal. BP. It is important to stress that more radiocarbon dates are on the way to help in this interpretation since the young age in GH2 is based only on a single sample.

Discussion

On current evidence, we can identify multiple events of Neanderthal local extinctions—first, a Neanderthal group, unrelated to later local populations, becomes extinct in the Altai during Marine Isotope Stage (MIS) 5 (130,000–74,000 BP) [11, 12], second, the extinction of a

Table 4. All lithic artifacts from the East trench.

Z	Flake	blade	Bladelet	Levallois blade	Levallois flake	core	tool	AD	SD/MD	sum
19.4–19.49	4	1							4	9
19.3–19.39										0
19.2–19.29										0
19.1–19.19	11		7			1	6	1	3	29
19.0–19.09	31	2	10				13	1	30	87
18.9–18.99	69	5	16			3	29	3	29	154
18.8–18.89	69	13	23			3	32	2	33	175
18.7–18.79	80	19	32			4	15	4	28	182
18.6–18.69	135	16	57			3	22	7	42	282
18.5–18.59	136	1	67			8	20	7	61	300
18.4–18.49	230	37	71			7	27	13	194	579
18.3–18.39	164	25	48	1		5	19	3	136	401
18.2–18.29	159	20	34		1	8	19	3	149	393
18.1–18.19	205	16	30		1	6	23	10	135	426
18.0–18.09	172	17	18			4	10	8	128	357
17.9–17.99	149	15	15			3	21	5	105	313
17.8–17.89	106	5	10			4	16	9	67	217
17.7–17.79	70	8	11				18	2	46	155
17.6–17.69	59	4	3			2	6	3	29	106
17.5–17.59	28	2	1				2		11	44
17.4–17.49	14	4	1		1		8	2	13	43
17.3–17.39	7						1		4	12
17.2–17.29	10						4	2	7	23
17.1–17.19	11		1				2		7	21
17.0–17.09	8		1				3		2	14
16.9–16.99	12		0	1			2		9	24
16.8–16.89	5		2						4	11
16.7–16.79	1						3	1	6	11
16.6–16.69	21		1				1		14	37
16.5–16.59	14		1				1		10	26
16.4–16.49	19	2					2	3	28	54
16.3–16.39	48	3					2	4	80	137
16.2–16.29	41	3	1			1	5		35	86
16.1–16.19	12		5				5	1	9	32
16.0–16.09	10		1					1	4	16
15.9–15.99	6	1							5	12
15.8–15.89	39	1	2		2	2	10	4	48	108
15.7–15.79	86	1	4	1	2		8	3	73	178
15.6–15.69	188	7	4		2	2	27	2	261	493
15.5–15.59	152	10	15	2	4	1	21	10	255	470
15.4–15.49	175	7	6	1	4	1	26	8	153	381
15.3–15.39	249	6	12		5	1	35	9	173	490
15.2–15.29	241	9	13	1	10		24	11	111	420
15.1–15.19	196	5	5		5		29	6	78	324
15.0–15.09	50	2	1	1	2		10	1	28	95
14.9–14.99	55	2	1		1	1	9	5	17	91
14.8–14.89	40	2					5	3	15	65

(Continued)

Table 4. (Continued)

Z	Flake	blade	Bladelet	Levallois blade	Levallois flake	core	tool	AD	SD/MD	sum
14.7–14.79	30	2				1	12		13	58
14.6–14.69	55	3	1	1		2	10		14	86
14.5–14.59	52	2	1	2	1	1	16		12	87
14.4–14.49	11		1				2	1	11	26
14.3–14.39	1						1		2	4
14.15–14.3	2								1	3
Sum	3738	278	533	11	41	74	582	158	2732	8151

The lithic artifacts are divided into technological categories based on artificial 10 cm spit. AD: angular debris, SD: small debitage (> 10mm), MD: micro debitage (> 5mm).

<https://doi.org/10.1371/journal.pone.0253708.t004>

different population of Neanderthals in the Altai between 59,000 and 49,000 BP [11, 12] that may overlap with the local disappearance of a Neanderthal population in the Crimea [50]; third, the disappearance of Neanderthals from the Levant by 48,000–49,000 BP [20], followed by a final event of the approximately synchronous disappearance of Neanderthal populations across a vast territory—from Western Europe to the Caucasus—between 40,000 and 37,000 BP

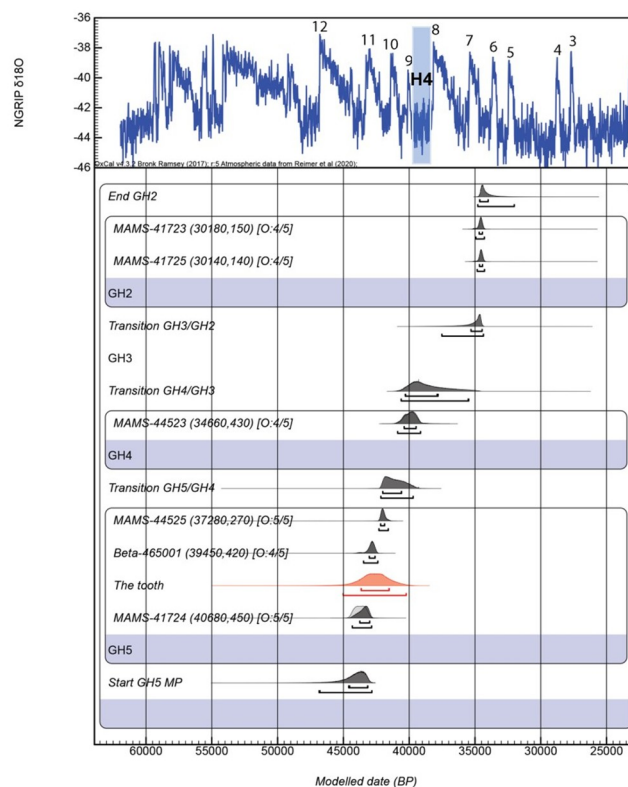


Fig 8. Bayesian model of Bawa Yawan rockshelter. Radiocarbon dates are calibrated using IntCal20 [43]; the model and boundaries were calculated using OxCal 4.3, including a General t-type Outlier Model [49]. Outliers prior and posterior probability are shown in square brackets. The chronology is compared to the North Greenland Ice Core Project (NGRIP) Greenland Ice Core Chronology 2005 (GICC05) $\delta^{18}\text{O}$ palaeo-environmental record [50] with warm Dansgaard-Oeschger events (from 12 to 3) and Heinrich stadial 4(H4).

<https://doi.org/10.1371/journal.pone.0253708.g008>

Table 5. Table shows the ¹⁴C dates available for the Bawa Yawan rockshelter sequence and of BY1 tooth, with its respective position in the layer (Column Z).

N	Period GH	QU	Z	GH	MPI Code	Lab. Code	Calibrated ¹⁴ C ages (cal. BP)	1s Err
1	Epi	E13	20.47	2	R-EVA 3304	MAMS-41722	11516	37
2	UP	I29	18.37	2	R-EVA 3299	MAMS-41721	-1535	19
3	UP	I29	18.12	2	R-EVA 3308	MAMS-41727	76	20
4	UP	I29	18.09	2	R-EVA 3452	MAMS-44524	-53	19
5	UP	G27	18.07	2	R-EVA 3292	MAMS-41723	30180	150
6	UP	G27	18.04	2	R-EVA 3295	MAMS-41725	30140	140
7	UP	I29	17.77	3	R-EVA 3296	MAMS-41726	-265	20
**8	MP	I31	16.16	4	R-EVA 3451	MAMS-44523	34660	430
9	MP	I31	15.93	5	R-EVA 3453	MAMS-44525	37280	270
10	MP	H31	15.88	5	Beta-465001	Beta-465001	39450	420
	BY1	I31	15.86	5	-	-	-	-
11	MP	I29	15.77	5	R-EVA 3300	MAMS-41724	40680	450
12	MP	H31	15.75	5		OxA-36752	>44200	-

<https://doi.org/10.1371/journal.pone.0253708.t005>

[2, 4, 22]. Contrasting with the synchronicity of their final disappearance, these late Neanderthal groups appear to be spatially structured and to have different demographic trajectories.

The discoveries from the Bawa Yawan rockshelter bring clarity to the position of the Zagros Mountains in this emerging picture. The presence of Neanderthals in the Zagros has been known for decades [26, 27, 29, 32]. However, few sites (Shanidar, Warwasi, Ghar-e-Khar, Kaldar, Ghamari, Gilvaran) preserve both MP and UP industries [25–27, 51, 52], while chronometric ages derive only from the old and new excavations at Shanidar, which point to the use of the cave by Neanderthals between 70,000 and 45,000 BP [26–28]. The age between 43,000 and 41,000 cal. BP for BY1 tooth associated with the Zagros Mousterian artifacts in the West-

Table 6. Bayesian Modelled calibrated ages and boundaries of Model 1 provided by the IntCal20 using OxCal 4.3 program [43, 49]. In red is the indirect date of the BY1 tooth provided by the 'date' command in OxCal.

Bawa Yawan rockshelter	Un-Modelled (BP)				Modelled (BP)			
	cal. BP 68.2%		cal. BP 95.4%		cal. BP 68.2%		cal. BP 95.4%	
Indices Amodel 108.2 Aoverall 107	from	To	from	To	From	To	from	to
End GH2					34650	34000	34790	32010
MAMS-41723 (30180;150)	34700	34410	35050	34290	34680	34440	34940	34280
MAMS-41725 (30140;140)	34660	34400	34900	34240	34660	34430	34840	34270
GH2								
Transition GH3/GH2					35310	34460	37520	34350
GH3								
Transition GH4/GH3					40300	37800	40610	35470
MAMS-44523 (34660;430)	40310	39400	40860	39080	40390	39470	40880	39130
GH4								
Transition GH5/GH4					42010	40570	42150	39700
MAMS-44525 (37280;270)	42160	41850	42270	41570	42180	41870	42300	41580
Beta-465001 (39450;420)	43050	42590	43850	42400	43030	42590	43470	42380
BY1					43660	41520	45030	40220
MAMS-41724 (40680;450)	44150	43280	44460	43000	43750	43000	44330	42850
GH5								
Start GH5 MP					44600	43140	46850	42830

<https://doi.org/10.1371/journal.pone.0253708.t006>

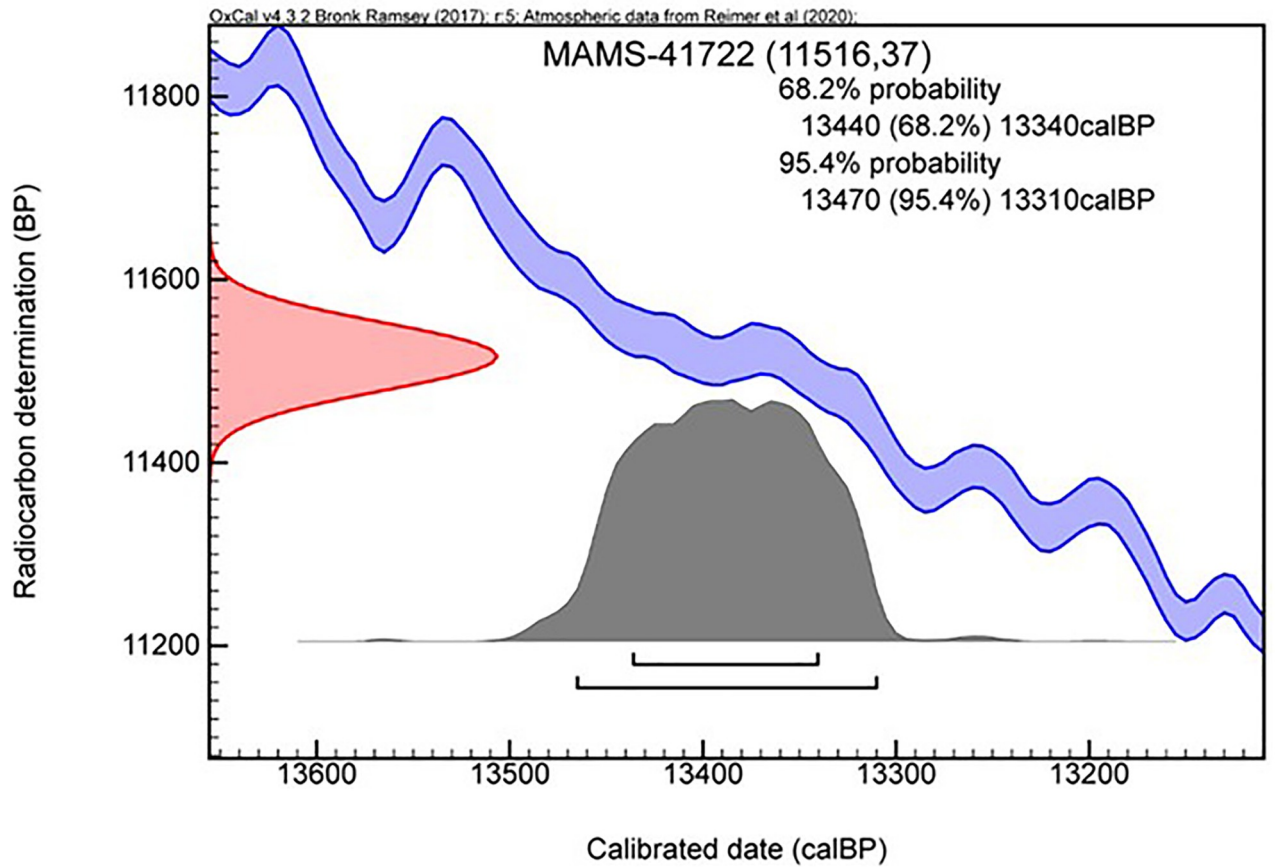


Fig 9. Calibrated radiocarbon date of Epipaleolithic layer in eastern trench of the Bawa Yawan rockshelter used IntCal20 in OxCal 4.3 program.

<https://doi.org/10.1371/journal.pone.0253708.g009>

Central Zagros revealed the presence of the Neanderthals at least until around 41,000 cal. BP. The Zagros Mousterian techno-complex continues above BY1 in GHs 4 and 3. However, in the lack of any hominin physical remains, yet it is not possible to evaluate the hominin type in these GHs and this remains an open hypothesis awaits further findings. The new data of Bawa

Table 7. Bayesian modelled boundaries and duration of the phases provided by the IntCal20¹³ using OxCal 4.3 program [49].

	Modelled (BP)			
	cal. BP 68.2%		cal. BP 95.4%	
	from	To	From	To
End GD2	34650	34000	34790	32010
Total Duration of GH2	34960	34220	36620	33000
Transition GD3/GD2	35310	34460	37520	34350
Transition GD4/GD3	40300	37800	40610	35470
Total Duration of GH4	41110	39090	41840	37320
Transition GD5/GD4	42010	40570	42150	39700
Transition GD5/GD4	42010	40570	42150	39700
Total Duration of GH5	43670	41540	45020	40210
Start GD5 MP	44600	43140	46850	42830

<https://doi.org/10.1371/journal.pone.0253708.t007>

Yawan together with the information from southern Caucasus [21, 23] suggest that caves and rockshelters throughout the entire mountains arch that extends from Georgia to Iran were used by relict population of Neanderthals could survived a short time after they had become extinct across most of Europe.

Furthermore, similar to the records of the Levant and Europe, the Zagros early UP assemblages are techno-typologically diverse, showing variable patterns of similarities and differences to early UP industries elsewhere, and suggesting a diversity of modern human groups with varying foraging strategies and ranges along the vast mountain chain [53]. The Bawa Yawan discoveries hypothesizes that the final disappearance of Neanderthals took place in the context of increasing competition with *Homo sapiens*, the multiple events of localised Neanderthal extinction, together with increasing genomic evidence of comparatively smaller population sizes in marginal areas [11]. The combination of these differences in demographic resilience between the two groups during periods of repeated climatic insults [54, 55], coupled with the more sophisticated technology of expanding modern humans (e.g., [56, 57] may have been the tipping point that created what appears as a vast spatial extinction event across thousands of kilometres, but was the sum of numerous local independent population processes, among which the disappearance of Neanderthals in the Zagros Mountains was one of the last. Finally, it will always be the case that artefactual data will be far more abundant than fossil evidence. Yet, as recent work in Central Asia and Siberia has shown [12], there are localised regional signatures among MP industries that may reflect cultural traditions associated with particular populations.

The sediment characteristics of this GH suggest a rather warm climate (comparing to the other GHs) leading to a more diverse fauna to appear in the environment. Unfortunately, due to the lack of high-resolution, well-dated paleoclimate records from the Zagros Mountains for the past 45,000 years, correlating our GHs to past regional climate changes is difficult. However, pollen evidence from Lake Zeribar characterised by high percentages of *Artemisa* and *Chenopodiaceae* indicates the dominance of a cool, dry steppe for the period between 40,000 and 14,000 cal. BP. Nevertheless, a slight increase in tree pollen at around 40,000 BP suggests a fairly warmer and wetter (less cold) climate at this time [58], which may correspond to the upper part of GH5.

Sediment compositions of GH4 and GH3 suggesting a prominent cold period characterized by higher snowfall simultaneous with Heinrich Stadial 4 (Figs 3B and 3C and 9). The highly calcareous nature of the sediments might point to an increase in the rate of chemical weathering due to the contact of snow meltwater with the surrounding limestone. One might speculate that the discharge of meltwater runoff rich in calcium carbonate into the rockshelter deposits has caused the highly calcareous sediments here. Moreover, the observed limestone fragments might originate from physical glacial erosion and permafrost degradation. Several lines of evidence such as a deep depression of the snowline to an elevation of about 1800 m in the Zagros Mountains during glacial periods [59], the enhanced rate of calcium carbonate deposition in the nearby Hashilan Wetland during cold climate intervals [60], and extremely sensitive climate of the West Asia to Heinrich cold events [61] provide supporting evidence for our interpretation that the observed highly calcareous sediments in this GH are associated with cold climatic conditions during Heinrich Stadial 4. Pollen evidence from Lake Zeribar reflects an almost treeless environment for the Zagros Mountains between ca. 33,000 and 15,000, which has been attributed to a colder and drier climate [58]. Given a considerable time gap at the transition from GH2 to GH1, it can be postulated that an intervening horizon has most likely been disappeared due to human interferences in the rockshelter environment.

The MP-UP transition in Europe which started between 47 kya BP overlapped with the spread of *Homo sapiens* and Neanderthals around 40 kya. Recent Palaeogenetic studies show

that the gene flow between Neanderthals and *Homo sapiens* have occurred in roughly between 60–50 probably in southwestern Asia [62, 63]. This new information is consistent with the data from Bawa Yawan. The Bawa Yawan Neanderthal suggests an extirpation date of around 45,000–40,000 cal. BP, but the lithic evidence shows extend for a while. If the conditions under which Neanderthals became extinct, locally and overall, are to be determined, it is necessary to develop a more integrated approach to the problem.

Conclusion and implications

The discovery of an *in situ* Neanderthal tooth at the Bawa Yawan rockshelter in the West-Central Zagros Mountains, its direct association with typical Zagros Mousterian artifacts, and the chronological attempt of the local MP to UP transition, has implications for our understanding of the spatial patterning of Neanderthal extinction and its relationship to expanding *Homo sapiens* populations and further work need to be done in order to shed more light on this intriguing region. In addition to expose a sequence of three archaeological techno-complexes of MP, UP and Epipalaeolithic formed in four GHs, excavations in Bawa Yawan rockshelter offer evidence that Neanderthals had a demographically dynamic history, shaped by multiple dispersal events and localised population extinctions. Since there is reliable evidence for diverse *Homo sapiens* in the Middle East during past 45,000, the last Zagros Neanderthals potentially overlapped with groups in space and time.

Acknowledgments

We are grateful to T. Higham, K. Douka, who kindly provided radiocarbon dating (sample number OxA-36752) for this project, and for useful discussion on the paper. We thank to a number of people who assisted us on this project late M. Azarnoosh, Y. Moradi, H. Chubak, A. Tahmasebi, F. Biglari, R. Shirazi (Iranian Center for Archaeological Research), B. Omrani (Research Institute of Cultural Heritage and Tourism), A. Gillies, K. Janin, N. Heydari, A. Tahmasebi, S. Kermajani, G. Weniger, R. Azizi, N. Naderian, E. Fotuhi, more specifically the excavation crew, the Heydari family and the local residents of Yawan village.

Author Contributions

Conceptualization: Saman Heydari-Guran.

Data curation: Saman Heydari-Guran, Stefano Benazzi, Sahra Talamo, Nemat Hariri, Robert A. Foley.

Formal analysis: Saman Heydari-Guran.

Funding acquisition: Saman Heydari-Guran.

Investigation: Saman Heydari-Guran, Stefano Benazzi, Sahra Talamo, Elham Ghasidian, Nemat Hariri, Faramarz Azizi, Rahmat Naderi, Reza Safaierad, Robert A. Foley.

Methodology: Saman Heydari-Guran, Stefano Benazzi, Sahra Talamo, Elham Ghasidian, Gregorio Oxilia, Jean-Jacques Hublin.

Project administration: Saman Heydari-Guran.

Resources: Saman Heydari-Guran.

Software: Saman Heydari-Guran, Stefano Benazzi, Sahra Talamo, Gregorio Oxilia.

Supervision: Saman Heydari-Guran.

Validation: Saman Heydari-Guran.

Visualization: Saman Heydari-Guran, Sahra Talamo, Gregorio Oxilia, Samran Asiabani, Faramarz Azizi.

Writing – original draft: Saman Heydari-Guran, Stefano Benazzi, Sahra Talamo, Elham Ghassidian, Reza Safaierad, Robert A. Foley, Marta M. Lahr.

Writing – review & editing: Saman Heydari-Guran, Stefano Benazzi.

References

1. Hublin JJ, Sirakov N, Aldeias V, Bailey S, Bard E, Delvigne V, et al. Initial upper palaeolithic homo sapiens from bacho kiro cave, Bulgaria. *Nature*. 2020 May; 581(7808):299–302.
2. Higham T, Douka K, Wood R, Ramsey CB, Brock F, Basell L, et al. The timing and spatiotemporal patterning of Neanderthal disappearance. *Nature*. 2014 Aug; 512(7514):306–9. <https://doi.org/10.1038/nature13621> PMID: 25143113
3. Talamo S, Aldeias V, Goldberg P, Chiotti L, Dibble HL, Guérin G, et al. The new 14C chronology for the Palaeolithic site of La Ferrassie, France: the disappearance of Neanderthals and the arrival of Homo sapiens in France. *Journal of Quaternary Science*. 2020 Oct; 35(7):961–73.
4. Zilhão J, Anesin D, Aubry T, Badal E, Cabanes D, Kehl M, et al. Precise dating of the Middle-to-Upper Paleolithic transition in Murcia (Spain) supports late Neandertal persistence in Iberia. *Heliyon*. 2017 Nov 1; 3(11):e00435. <https://doi.org/10.1016/j.heliyon.2017.e00435> PMID: 29188235
5. Benazzi S, Douka K, Fornai C, Bauer CC, Kullmer O, Svoboda J, et al. Early dispersal of modern humans in Europe and implications for Neanderthal behaviour. *Nature*. 2011 Nov; 479(7374):525–8. <https://doi.org/10.1038/nature10617> PMID: 22048311
6. Benazzi S, Slon V, Talamo S, Negrino F, Peresani M, Bailey SE, et al. The makers of the Protoaurignacian and implications for Neandertal extinction. *Science*. 2015 May 15; 348(6236):793–6. <https://doi.org/10.1126/science.aaa2773> PMID: 25908660
7. Fu Q, Hajdinjak M, Moldovan OT, Constantin S, Mallick S, Skoglund P, et al. An early modern human from Romania with a recent Neandertal ancestor. *Nature*. 2015 Aug; 524(7564):216–9. <https://doi.org/10.1038/nature14558> PMID: 26098372
8. Hublin JJ. The last Neanderthal. *Proceedings of the National Academy of Sciences*. 2017 Oct 3; 114(40):10520–2. <https://doi.org/10.1073/pnas.1714533114> PMID: 28973864
9. Picin A, Hajdinjak M, Nowaczewska W, Benazzi S, Urbanowski M, Marciszak A, et al. New perspectives on Neanderthal dispersal and turnover from Stajnia Cave (Poland). *Scientific reports*. 2020 Sep 8; 10(1):1–2. <https://doi.org/10.1038/s41598-019-56847-4> PMID: 31913322
10. Krause J, Orlando L, Serre D, Viola B, Prüfer K, Richards MP, et al. Neanderthals in central Asia and Siberia. *Nature*. 2007 Oct; 449(7164):902–4. <https://doi.org/10.1038/nature06193> PMID: 17914357
11. Mafessoni F, Grote S, de Filippo C, Slon V, Kolobova KA, Viola B, et al. A high-coverage Neandertal genome from Chagyrskaya Cave. *Proceedings of the National Academy of Sciences*. 2020 Jun 30; 117(26):15132–6. <https://doi.org/10.1073/pnas.2004944117> PMID: 32546518
12. Kolobova KA, Roberts RG, Chabai VP, Jacobs Z, Krajcarz MT, Shalagina AV, et al. Archaeological evidence for two separate dispersals of Neanderthals into southern Siberia. *Proceedings of the National Academy of Sciences*. 2020 Feb 11; 117(6):2879–85. <https://doi.org/10.1073/pnas.1918047117> PMID: 31988114
13. Prüfer K, Racimo F, Patterson N, Jay F, Sankararaman S, Sawyer S, et al. The complete genome sequence of a Neanderthal from the Altai Mountains. *Nature*. 2014 Jan; 505(7481):43–9.
14. Petraglia MD, Alsharekh A, Breeze P, Clarkson C, Crassard R, Drake NA, et al. Hominin dispersal into the Nefud desert and Middle Palaeolithic settlement along the Jubbah palaeolake, northern Arabia. *PLoS One*. 2012 Nov 19; 7(11):e49840. <https://doi.org/10.1371/journal.pone.0049840> PMID: 23185454
15. Lahr MM, Foley R. Multiple dispersals and modern human origins. *Evolutionary Anthropology: Issues, News, and Reviews*. 1994; 3(2):48–60.
16. Hershkovitz I, Weber GW, Quam R, Duval M, Grün R, Kinsley L, et al. The earliest modern humans outside Africa. *Science*. 2018 Jan 26; 359(6374):456–9. <https://doi.org/10.1126/science.aap8369> PMID: 29371468

17. Mercier N, Valladas H, Bar-Yosef O, Vandermeersch B, Stringer C, Joron JL. Thermoluminescence date for the Mousterian burial site of Es-Skhal, Mt. Carmel. *Journal of Archaeological Science*. 1993 Mar 1; 20(2):169–74.
18. Hershkovitz I, Marder O, Ayalon A, Bar-Matthews M, Yasur G, Boaretto E, et al. Levantine cranium from Manot Cave (Israel) foreshadows the first European modern humans. *Nature*. 2015 Apr; 520(7546):216–9. <https://doi.org/10.1038/nature14134> PMID: 25629628
19. Valladas H, Joron JL, Valladas G, Arensburg B, Bar-Yosef O, Belfer-Cohen A, et al. Thermoluminescence dates for the Neanderthal burial site at Kebara in Israel. *Nature*. 1987 Nov; 330(6144):159–60.
20. Abadi I, Bar-Yosef O, Belfer-Cohen A. Kebara V—A Contribution for the Study of the Middle-Upper Paleolithic Transition in the Levant. *PaleoAnthropology*. 2020:1–28.
21. Adler DS, Bar-Yosef O, Belfer-Cohen A, Tushabramishvili N, Boaretto E, Mercier N, et al. Dating the demise: Neanderthal extinction and the establishment of modern humans in the southern Caucasus. *Journal of Human Evolution*. 2008 Nov 1; 55(5):817–33. <https://doi.org/10.1016/j.jhevol.2008.08.010> PMID: 18930307
22. Pinhasi R, Thomas MG, Hofreiter M, Currat M, Burger J. The genetic history of Europeans. *Trends in Genetics*. 2012 Oct 1; 28(10):496–505. <https://doi.org/10.1016/j.tig.2012.06.006> PMID: 22889475
23. Adler DS, Tushabramishvili NI. Middle Palaeolithic patterns of settlement and subsistence in the southern Caucasus. *Middle Palaeolithic settlement dynamics*. 2004:91–132.
24. Yousefi M, Heydari-Guran S, Kafash A, Ghasidian E. Species distribution models advance our knowledge of the Neanderthals' paleoecology on the Iranian plateau. *Scientific reports*. 2020 Aug 28; 10(1):1–9.
25. Smith PE. *Palaeolithic archaeology in Iran*. American Institute of Iranian Studies; 1986.
26. Solecki RS. Prehistory in Shanidar valley, northern Iraq. *Science*. 1963 Jan 18; 139(3551):179–93. <https://doi.org/10.1126/science.139.3551.179> PMID: 17772076
27. Pomeroy E, Lahr MM, Crivellaro F, Farr L, Reynolds T, Hunt CO, et al. Newly discovered Neanderthal remains from Shanidar Cave, Iraqi Kurdistan, and their attribution to Shanidar 5. *Journal of Human Evolution*. 2017 Oct 1; 111:102–18. <https://doi.org/10.1016/j.jhevol.2017.07.001> PMID: 28874265
28. Pomeroy E, Hunt CO, Reynolds T, Abdulmutalib D, Asouti E, Bennett P, et al. Issues of theory and method in the analysis of Paleolithic mortuary behavior: A view from Shanidar Cave. *Evolutionary Anthropology: Issues, News, and Reviews*. 2020 Sep; 29(5):263–79. <https://doi.org/10.1002/evan.21854> PMID: 32652819
29. Zanolli C, Biglari F, Mashkour M, Abdi K, Monchot H, Debue K, et al. A Neanderthal from the Central Western Zagros, Iran. Structural reassessment of the Wezmeh 1 maxillary premolar. *Journal of human evolution*. 2019 Oct 1; 135:102643. <https://doi.org/10.1016/j.jhevol.2019.102643> PMID: 31421316
30. Becerra-Valdivia L, Douka K, Comeskey D, Bazgir B, Conard NJ, Marean CW, et al. Chronometric investigations of the Middle to Upper Paleolithic transition in the Zagros Mountains using AMS radiocarbon dating and Bayesian age modelling. *Journal of human evolution*. 2017 Aug 1; 109:57–69. <https://doi.org/10.1016/j.jhevol.2017.05.011> PMID: 28688460
31. Heydari-Guran S, Douka K, Higham T, Münzel SC, Deckers K, Hourshid S, et al. Early Upper Palaeolithic occupation at Gelimgoush cave, Kermanshah; West-Central Zagros mountains of Iran. *Journal of Archaeological Science: Reports*. 2021; 38:103050.
32. Coon CS. *Cave Explorations in Iran 1949*, Museum Monographs, the University Museum, University of Pennsylvania, Philadelphia. 1951.
33. Heydari-Guran S, Ghasidian E. Late Pleistocene hominin settlement patterns and population dynamics in the Zagros Mountains: Kermanshah region. *Archaeological Research in Asia*. 2020 Mar 1; 21:100161.
34. Turner CI. Scoring produces for key morphological traits of the permanent dentition: The Arizona State University dental anthropology system. *Advances in dental anthropology*. 1991:13–31.
35. Arnaud J, Peretto C, Panetta D, Tripodi M, Fontana F, Arzarello M, et al. A reexamination of the Middle Paleolithic human remains from Riparo Tagliente, Italy. *Quaternary International*. 2016 Dec 15; 425:437–44.
36. Margherita C, Oxilia G, Barbi V, Panetta D, Hublin JJ, Lordkipanidze D, et al. Morphological description and morphometric analyses of the Upper Palaeolithic human remains from Dzudzuana and Satsurbliia caves, western Georgia. *Journal of human evolution*. 2017 Dec 1; 113:83–90. <https://doi.org/10.1016/j.jhevol.2017.07.011> PMID: 29054170
37. Romandini M, Oxilia G, Bortolini E, Peyrégne S, Delpiano D, Nava A, et al. A late Neanderthal tooth from northeastern Italy. *Journal of Human Evolution*. 2020 Oct 1; 147:102867. <https://doi.org/10.1016/j.jhevol.2020.102867> PMID: 32889336

38. Molnar S. Human tooth wear, tooth function and cultural variability. *American Journal of Physical Anthropology*. 1971 Mar; 34(2):175–89. <https://doi.org/10.1002/ajpa.1330340204> PMID: 5572602
39. Moorrees CF, Fanning EA, Hunt EE Jr. Formation and resorption of three deciduous teeth in children. *American Journal of Physical Anthropology*. 1963 Jun; 21(2):205–13. <https://doi.org/10.1002/ajpa.1330210212> PMID: 14110696
40. Foster TD, Hamilton MC, Lavelle CL. Dentition and dental arch dimensions in British children at the age of 212 to 3 years. *Archives of oral biology*. 1969 Sep 1; 14(9):1031–40. [https://doi.org/10.1016/0003-9969\(69\)90073-9](https://doi.org/10.1016/0003-9969(69)90073-9) PMID: 5259648
41. Benazzi S, Panetta D, Fornai C, Toussaint M, Gruppioni G, Hublin JJ. Guidelines for the digital computation of 2D and 3D enamel thickness in hominoid teeth. *American Journal of Physical Anthropology*. 2014 Feb; 153(2):305–13. <https://doi.org/10.1002/ajpa.22421> PMID: 24242830
42. Crevecoeur I, Bayle P, Rougier H, Maureille B, Higham T, van der Plicht J, et al. The Spy VI child: A newly discovered Neanderthal infant. *Journal of Human Evolution*. 2010 Dec 1; 59(6):641–56. <https://doi.org/10.1016/j.jhevol.2010.07.022> PMID: 20934740
43. Kromer B, Lindauer S, Synal HA, Wacker L. MAMS—a new AMS facility at the Curt-Engelhorn-Centre for Archaeometry, Mannheim, Germany. *Nuclear instruments and methods in physics research Section B: beam interactions with materials and atoms*. 2013 Jan 1; 294:11–3.
44. Reimer PJ, Austin WE, Bard E, Bayliss A, Blackwell PG, Ramsey CB, et al. The IntCal20 Northern Hemisphere radiocarbon age calibration curve (0–55 cal kBP). *Radiocarbon*. 2020 Aug; 62(4):725–57.
45. AlQahtani SJ, Hector MP, Liversidge HM. Brief communication: the London atlas of human tooth development and eruption. *American Journal of physical anthropology*. 2010 Jul; 142(3):481–90. <https://doi.org/10.1002/ajpa.21258> PMID: 20310064
46. Ghasidian E. Rethinking the Upper Palaeolithic of the Zagros Mountains. *Paleo Anthropol*. 2019:240–310.
47. Olszewski DI. The Zarzian Occupation at Warwasi Rockshelter, Iran. In *The Paleolithic Prehistory of the Zagros-Taurus* 1993 Jan 29 (Vol. 83, pp. 207–217). The University Museum, University of Pennsylvania.
48. Dibble HL, Holdaway SJ. The Middle Paleolithic industries of Warwasi. *The Paleolithic Prehistory of the Zagros-Taurus*. 1993 Jan 29:75–99.
49. Ramsey C.B., 2009. Dealing with outliers and offsets in radiocarbon dating. *Radiocarbon*, 51 (3), pp.1023–1045.
50. Svensson A, Andersen KK, Bigler M, Clausen HB, Dahl-Jensen D, Davies SM, et al. A 60 000 year Greenland stratigraphic ice core chronology. *Climate of the Past*. 2008 Mar 31; 4(1):47–57.
51. Hajdinjak M, Fu Q, Hübner A, Petr M, Mafessoni F, Grote S, et al. Reconstructing the genetic history of late Neanderthals. *Nature*. 2018 Mar; 555(7698):652–6. <https://doi.org/10.1038/nature26151> PMID: 29562232
52. Bazgir B, Ollé A, Tumung L, Becerra-Valdivia L, Douka K, Higham T, et al. Understanding the emergence of modern humans and the disappearance of Neanderthals: Insights from Kaldar Cave (Khorramabad Valley, Western Iran). *Scientific reports*. 2017 Mar 2; 7(1):1–6.
53. Bazgir B, Otte M, Tumung L, Ollé A, Deo SG, Joglekar P, et al. Test excavations and initial results at the middle and upper Paleolithic sites of Gilvaran, Kaldar, Ghamari caves and Gar Arjene Rockshelter, Khorramabad Valley, western Iran. *Comptes Rendus Palevol*. 2014 Sep 1; 13(6):511–25.
54. Ghasidian E, Heydari-Guran S, Lahr MM. Upper Paleolithic cultural diversity in the Iranian Zagros Mountains and the expansion of modern humans into Eurasia. *Journal of human evolution*. 2019 Jul 1; 132:101–18. <https://doi.org/10.1016/j.jhevol.2019.04.002> PMID: 31203842
55. Columbu A, Chiarini V, Spötl C, Benazzi S, Hellstrom J, Cheng H, et al. Speleothem record attests to stable environmental conditions during Neanderthal–modern human turnover in southern Italy. *Nature ecology & evolution*. 2020 Sep; 4(9):1188–95.
56. Staubwasser M, Drăguşin V, Onac BP, Assonov S, Ersek V, Hoffmann DL, et al. Impact of climate change on the transition of Neanderthals to modern humans in Europe. *Proceedings of the National Academy of Sciences*. 2018 Sep 11; 115(37):9116–21. <https://doi.org/10.1073/pnas.1808647115> PMID: 30150388
57. Sano K, Arrighi S, Stani C, Aureli D, Boschin F, Fiore I, et al. The earliest evidence for mechanically delivered projectile weapons in Europe. *Nature ecology & evolution*. 2019 Oct; 3(10):1409–14. <https://doi.org/10.1038/s41559-019-0990-3> PMID: 31558829
58. Van Zeist W, Bottema S. Palynological investigations in western Iran. *Palaeohistoria*. 1977 Dec 15:19–85.

59. Wright HE. Pleistocene glaciation in Kurdistan. *E&G Quaternary Science Journal*. 1962 Jan 15; 12(1):131–64.
60. Safaierad R, Azizi G, Maghsoudi M. The role of changes in the large-scale atmospheric systems in the evolution of the late Pleistocene and Holocene climate of the Zagros Mountains. *Quaternary Journal of Iran*. 2018 Dec 10; 4(3):253–71.
61. Safaierad R, Mohtadi M, Zolitschka B, Yokoyama Y, Vogt C, Schefuß E. Elevated dust depositions in West Asia linked to ocean–atmosphere shifts during North Atlantic cold events. *Proceedings of the National Academy of Sciences*. 2020; 117(31):18272–7. <https://doi.org/10.1073/pnas.2004071117> PMID: 32690680
62. Prüfer K, Posth C, Yu H, Stöessel A, Spyrou MA, Deviese T, et al. A genome sequence from a modern human skull over 45,000 years old from Zlatý kůň in Czechia. *Nature Ecology & Evolution*. 2021; 5(6):820–5 <https://doi.org/10.1038/s41559-021-01443-x> PMID: 33828249
63. Hajdinjak M, Mafessoni F, Skov L, Vernot B, Hübner A, Fu Q, et al. Initial Upper Palaeolithic humans in Europe had recent Neanderthal ancestry. *Nature*. 2021; 592(7853):253–7. <https://doi.org/10.1038/s41586-021-03335-3> PMID: 33828320